



ECG parameters to predict left ventricular electrical delay

Maria P. Bonomini^{a,b,*}, Daniel F. Ortega^{c,d}, Luis D. Barja^{c,d}, Emilio Logarzo^{c,d}, Nicolás Mangani^{c,d}, Analía Paolucci^{c,d}

^aInstituto de Ingeniería Biomédica, Facultad de Ingeniería, Universidad de Buenos Aires, Argentina

^bInstituto Argentino de Matemática, 'Alberto P. Calderón' CONICET, Buenos Aires, Argentina

^cClínica San Camilo, Buenos Aires, Argentina

^dHospital Universitario Austral, Buenos Aires, Argentina



ARTICLE INFO

Available online xxxx

Keywords:

Intraventricular dyssynchrony

ECG

Nonselective His Bundle pacing

Left Ventricular Electrical Delay

ABSTRACT

Aims: Left ventricular (LV) dyssynchrony lengthens the left ventricular electrical delay (LVED), measured from QRS onset to the first peak of the LV electrogram. We constructed an ECG model to predict LVED noninvasively.

Methods: Inpatient LVED was measured during a baseline vs nonselective His bundle pacing (nHBP) protocol. This setup provided paired synchronic/non-synchronic LVEDs, allowing inpatient comparisons. Crosscorrelation of leads II and V_6 was accomplished and extracted features together with age and gender fed a linear mixed effects model to predict LVED.

Results: Hemodynamic increments were consistent with LVED advances under nHBP in a subset of 17 patients (dp/dt_{max} , baseline: 938.82 ± 241.95 mm Hg/s vs nHBP: 1034.94 ± 253.63 mm Hg/s, $p = 6.24e-4$). The inclusion of the area under V_6 (A_{V_6}) and the time shift of R-peaks obtained from the crosscorrelation signal (Cor_S) grouped by patient significantly improved LVED estimation with respect to the model based only on QRS duration, age and gender ($p = 1.7e-5$).

Conclusions: Interlead ECG changes explained LVED, providing clues about the electrical impulse conduction within the left ventricle noninvasively.

© 2018 Elsevier Inc. All rights reserved.

Introduction

In the last three decades, a growing body of literature focused on alternative implementations for cardiac pacing, after a long period of right ventricular pacing (RVP) in apex. RVP has been shown to exert deleterious effects on cardiac function [1] and to create left bundle branch block (LBBB) patterns, delaying the electrical activation of the left ventricular lateral wall with respect to the interventricular septum [2]. Cardiac resynchronization therapy turned out to address this dyssynchronous activation, advancing the left ventricle activation by means of a lead placed via the coronary venous system. Even though CRT proved to improve mortality and non-fatal heart failure events, it still presents a high rate (about 30–40%) of non-responders [3,4]. Recently, it was reported the relationship between LVED and left ventricular remodelling with cardiac resynchronization therapy, postulating the optimal site for the LV lead as that with the latest LVED [5–7].

In contrast to RVP or CRT, the recent His bundle pacing (HBP) approach relies on the conduction paths of the cardiac system, emerging as the most physiological pacing strategy that allows restoration of native conduction in those patients with proximal His Purkinje disease [8–10]. However, certain technical and anatomical aspects still obscure the widespread of HBP, such as anatomical variations between patients, distal or complex blocks as the cause of dyssynchrony or appropriate catheters to target the small area of the His bundle. In fact, finding the optimal stimulation site can be a time-consuming task which may lead to intraoperative complications at implantation [11].

His bundle pacing has two possible mechanisms. It can capture directly the His bundle (selective His bundle) producing a latency equal to the His-ventricular interval and a QRS morphology identical to the intrinsic QRS complex. Nonselective His bundle pacing (nHBP), on the other hand, results from the fusion of the adjacent myocardium and the His bundle, producing a “delta-wave” that precedes the QRS complex. No matter whether selective or not, His bundle pacing advances the left ventricular activation, greatly improving intraventricular synchrony [12,13]. Therefore, it might be useful to construct a model based on those ECG parameters that explain LVED measures in order to assist in the noninvasive evaluation and/or

* Corresponding author at: Instituto Argentino de Matemática Alberto P. Calderón, CONICET, Buenos Aires, Argentina.

E-mail address: paula.bonomini@conicet.gov.ar (M.P. Bonomini).

optimization of cardiac stimulation devices or simply to assess cardiac dyssynchrony electrocardiographically. Furthermore, since QRS narrowing is not always possible with nHBP, noninvasive assessment of LVED could guide a quantitative search for the optimal pacing site.

Finally, we hypothesized that multi ECG lead would be better than single ECG lead variations to describe LVED. Therefore, an inter-lead signal derived from the crosscorrelation of electrocardiographic leads II and V₆ was constructed, on which we extracted temporal and morphological features, which served as inputs to a mixed-effects model for LVED during an acute basal vs nHBP protocol in 26 patients with conduction disease disturbances.

Materials and methods

Population study and stimulation protocol

We retrospectively studied de-identified data from 30 consecutive patients referred to electrophysiologic study (EP) for cardiode-fibrillator indication. Of these 30, 4 patients were excluded from analysis due to incomplete clinical records. Patients covered a wide range of conduction disturbances (see Table 1). Age ranged from 52 to 76 years old and subgroups were balanced for age and gender (chi-square = NS). Five ECG variables were obtained during a Basal vs nHB pacing protocol on these patients.

So as not to interfere with fluoroscopic images or to prolong EP time, only leads I, II, V₁ and V₆ were recorded. According to this setup, LBBB was defined as notched or broad slurred R waves in leads I and V₆, and rS or QS pattern in lead V₁. Analogously, RBBB was defined as rsr, rSR, or rSR morphology in V₁, and deep S waves in V₆ as recommended by AHA [14]. Consistently, nonspecific intraventricular conduction disturbance (NICD) patients accounted for the cases with moderate widened QRS where LBBB or RBBB definitions did not apply.

For electrical determination of dyssynchrony, a decapolar catheter with an interelectrode distance of 2.5–2.5 mm was inserted via the coronary sinus, considering the latest local bipolar electrogram for the measurement of the left ventricular activation. LVED was defined as the time elapsed from the beginning of surface QRS to the most distal left ventricular electrogram deflection recorded from coronary sinus in all patients [12].

nHBP was implemented biphasically with a phase width of 0.5 ms followed by a subthreshold recovery phase to avoid electrode polarization (overall pulse width of 1 ms). A specially designed, quad-configured pacing cable was connected to a Blazer II EPT 4 mm Boston Scientific stimulation catheter and a ground pad beneath the patient was utilized as reference for all four channels. For more detail about stimulation protocol refer to [13].

Finally, the study was approved by the Ethics Committee of the “ Instituto de Investigaciones Medicas Dr. Alfredo Lanari ”. In all cases, patients were thoroughly informed and provided written informed consent.

Table 1

Baseline characteristics of the population study according to QRS duration. EF: Ejection fraction. QRSd: QRS duration. LVED: left ventricular electrical delay. LBBB: left bundle branch block. NICD: nonspecific intraventricular conduction disturbance. AVB: AV block, 2nd degree.

Baseline patient characteristics	QRS _d > 120 ms	QRS _d < 120 ms
Age (y.o.)	65 ± 13	57 ± 19
Women	5 (38%)	8 (61%)
QRS _d (ms)	186.92 ± 19.31	139.46 ± 21.26*
LVED (ms)	115.23 ± 17.73	91.23 ± 27.24*
EF %	24	27
LBBB	18 (100%)	0
RBBB	0	4 (100%)
NICD	0	4 (100%)

* p < 0.05.

LVED estimation

Crosscorrelation is a measure of similarity of two signals as a function of the displacement of one relative to the other. In intrinsic conduction, simultaneous QRS complexes from different leads tend to minimize the phase between them. This is, R peaks tend to align themselves spatially (Fig. 1). However, when conduction paths are altered, leads projecting on fibrotic or non-conductive myocardium show delayed peaks, in addition to the changes in morphology that affect the similarity from the healthy situation. This is the foundation for the crosscorrelation analysis chosen in this study.

All possible permutations of two leads in the ensemble I-II-V₁-V₆ were analyzed. Only the pair providing the best fit, II-V₆, remained for further analysis (see Table 2). ECG recordings were bandpassed with a Butterworth filter (4th order, 0.5–80 Hz), power line interference was attenuated by means of a notch filter (Butterworth, 4th order, 50 Hz) and fiducial points were found by means of a wavelet-transform delineator [15]. Interlead features were extracted during depolarization, therefore, QRS segmentation was accomplished on both leads, being II^{QRS} and V₆^{QRS} the corresponding QRS segments consisting of a window of 300 samples (182 ms, sampling frequency = 1640 sps) starting at the median of every lead’s QRS onsets. Crosscorrelation was then applied to QRS segments. Characterization of the resulting correlation signal gave rise to the following parameters: 1) Maximum correlation amplitude (Cor_A) between leads II^{QRS} and V₆^{QRS}; estimating the average amplitude between leads II and V₆, 2) Correlation width (Cor_W) measured at 70% of maximum correlation amplitude; relating average QRS widths, 3) Correlation shift (Cor_S) measured at the peak time of the crosscorrelation signal (phase), 4) QRS duration (QRS_d) measured from spike to QRS latest offset when pacing, or from earliest QRS onset and latest QRS offset otherwise and 5) Area under V₆^{QRS} (A_{V₆}), with Crosscorrelation between II^{QRS} and V₆^{QRS} defined as

$$Xcor_{IIV_6}(m) = \sum_{i=1}^{300-m} II_{(i+m)}^{QRS} V_{6(i)}^{QRS} \tag{1}$$

The former ECG parameters plus QRS_d, age and gender were tested as predictors in a linear mixed model to assess their association with LVED.

Fig. 1 exemplifies the procedure of QRS segmentation (middle) and crosscorrelation feature extraction (right) from the acquired ECG leads (left) in a sinus rhythm ECG trace. Arrows indicate the QRS complexes on which the procedure was carried out. Notice that QRS peaks for those leads coincide in the heart with intact conduction, resulting in the crosscorrelation signal centered at time zero (Cor_S = 0). In order to contrast results obtained with this model, a second model based on QRS_d, age and gender was also constructed. For clarity sake, nomenclature was defined as follows: LVED will be used for the invasive quantity measured from coronary sinus, in contrast to LV ED_{ecg}, which will refer to the output of the ECG model and LV ED_{qrs}, referring to the output of the QRS model.

Statistical analysis

All data are expressed as mean ± SD. The D’Agostino-Pearson normality test was applied to quantify the discrepancy between the parameters distributions and an ideal Gaussian distribution. T-student test was used to compare paired data (Baseline against nHB). Gender distribution and age in the two patient subgroups were compared by chi square test. A two-sided p < 0.05 was regarded as significant. Since we are dealing with paired data, a mixed-effect model with subject as the grouping variable was evaluated by comparison between ECG and QRS models of Akaike, loglikelihood and BIC values. Also, the likelihood ratio test compared the significant

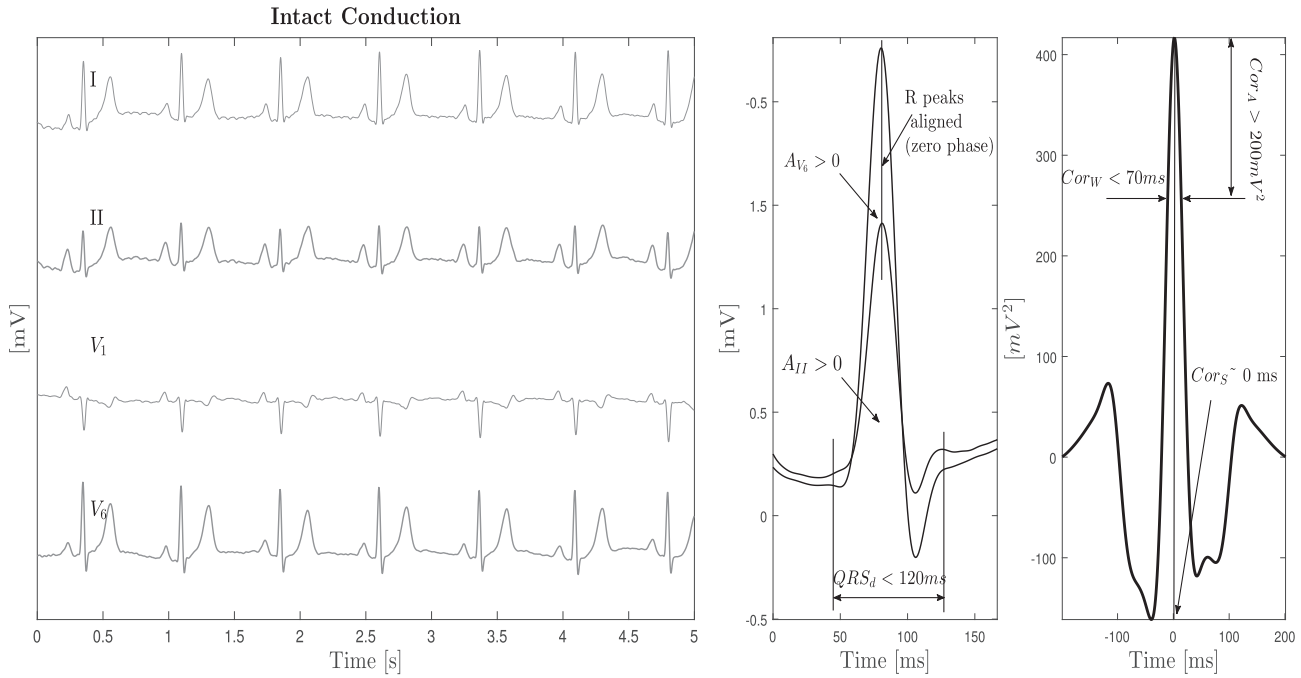


Fig. 1. Correlation analysis and normal values for a patient with intact intraventricular conduction on leads II and V₆. Left) ECG traces recorded during EP. Middle) Superimposed QRS segments (II^{QRS} and V_6^{QRS}). Right) Leads II and V₆ crosscorrelation. QRS peaks coincide and crosscorrelation signal shows its maximum at time zero ($Cor_S = 0$). Cor_S : Correlation shift (ms), Cor_W : Correlation width (ms), Cor_A : Correlation amplitude (mV), A_{II} : area under lead II, A_{V_6} : area under lead V₆.

improvement of the ECG over the QRS model. The mixed effects model parameters were estimated by the Maximum Likelihood (ML) method. Wilkinson notation was used, so that interaction terms were also included. Bland-Altman plots were constructed to determine the differences between measured and estimated LVED.

Results

Lead selection

Interlead variations were obtained by the crosscorrelation technique. Since crosscorrelation is a linear operation involving sums and inner products of one signal overimposing another signal, only two leads formed the interlead sets. The hypothesis underlying this work is that inferior and lateral leads, in particular leads II and V₆ account for the maximum variance of the activation front in the left ventricle. In this sense, lead II runs parallel to the septum while V₆ is the horizontal lead that better sees the left lateral wall. Then, the correlation of these two leads should properly detect any deviation from normality in situations where conduction paths are altered. In order to confirm this hypothesis, we have run the correlation analysis for other interlead sets grouped according to the ventricle portions they best describe, this is, inferior, left lateral and right lateral leads (Table 2). Results confirm the hypothesis, with the pair II-V₆ providing the best fit, measured by the adjusted coefficient of determination (Adjusted R²). Also, notice that the group of inferior-left

Table 2
Goodness of fit for different interlead sets grouped according to the portion of the ventricle they best describe. Inf-Left: inferior-left, Inf-Right: inferior-right. The inferior-left sets provided the best fits, with the leads II and V₆ originating the highest Adjusted R² (bold).

	Inf-Left			Inf-Right				Right-left	
Interlead set	I-II	I-III	III-V ₆	II-V₆	aV _F -V ₆	III-V ₁	II-V ₁	aV _F -V ₁	V ₁ -V ₆
Adjusted R ²	0.66	0.44	0.68	0.78	0.66	0.17	0.23	0.21	0.55

leads originated good fits in general while the group of inferior-right leads did not.

Crosscorrelation parameters

The mean ± SD values for the ECG parameters, together with response variable (LVED) analyzed during sinus rhythm (SR) and nHB pacing on leads II-V₆ are presented in Fig. 2. Note that both predictors and response were normalized through out basal and nHB pacing to allow a better simultaneous representation.

It is worth mentioning the advance of LVED (34.58 ± 24.61 ms in average) in accordance with QRS shortenings of 24.37 ± 28.56 ms during nHB pacing for patients with wide QRS (greater than 120 ms). However, this relationship did not hold for narrow QRS, where QRS shortening suffered slightly (-11.87 ± 16.88 ms) but not LVED advance (20.12 ± 23.48 ms). This could probably be attributed to the RBBB cases with preserved left ventricular conduction, where LVED showed no changes from SR to nHB.

Hemodynamical changes

In order to corroborate the beneficial effect induced by nHB pacing consistent with LVED improvement, we measured hemodynamical changes in a subset of 17 patients. LV pressure was recorded by means of a Millar pressure transducer under SR and nHB pacing. LV pressure was continuously monitored during 5 ON/OFF cycles of nHB paced and SR beats. LV dp/dt_{max} presented a higher level for nHB versus SR (1034.94 ± 253.63 mm Hg/s vs 938.82 ± 241.95 mm Hg/s, $p = 6.24e-4$), with individual raises in 14 patients, no change in one (a difference of 5 mm Hg/s or lesser) and decrease in two patients (see Table 3).

LVED estimation

Table 4 shows the model estimated coefficients together with the respective statistics for the fixed and random terms contributing to

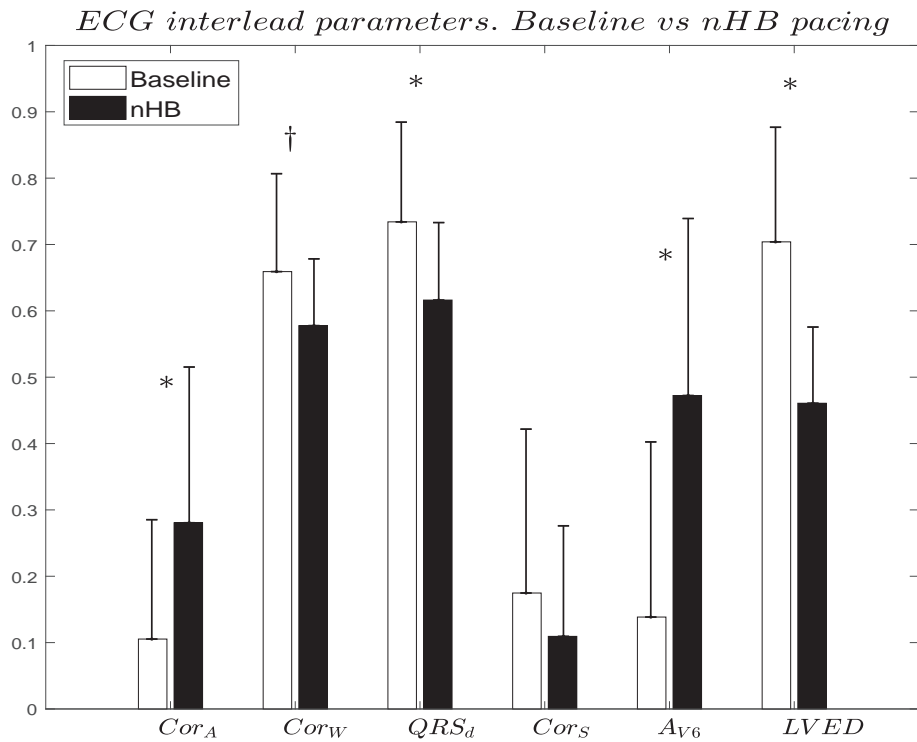


Fig. 2. Normalized mean \pm SD ECG parameters analyzed during sinus rhythm and nHB pacing on leads II-V₆. Cor_S: Correlation shift (ms), Cor_W: Correlation width (ms), Cor_A: Correlation amplitude (mV), AV₆: area under lead V₆, QRS_d: QRS duration (ms), LVED: left ventricular electrical delay, the response variable. *p < 0.0005, †p < 0.005.

the LVED_{ecg} model. Since QRS duration has been proved to be a significant determinant of CRT response [16], we estimated LVED with a second linear model based only on QRS duration, age and gender. Fig. 3 shows the differences in model performance for QRS and ECG models in two formats: the top panel displays measured vs estimated LVED correlations, while the bottom panel shows their respective Bland-Altman plots. The ECG regression (top left panel) produced an adjusted R² of 0.78 (AIC = 471.59) while the simple QRS_d regression (top right panel) gave an adjusted R² of 0.22 (AIC = 488.08). Additionally, the fixed effects showed small p-values while the 95% CI interval for the random effect was small and did not contain

zero, which means that grouping by patient significantly improved the regression. In order to compare the models, a likelihood ratio test was run and led to the same conclusion; the ECG model performed better than the QRS model at a significance of 1.7e-5. Table 5 shows this p-value together with a summary of the most important statistics associated to each model.

From observing Bland-Altman plots, it is clear that the ECG model presented an unbiased estimation (bottom left panel) while the QRS_d model showed a non-consistent bias throughout the average measures (bottom right panel), underestimating for short LVED values while overestimating for long LVED values. Also note the greater

Table 3

Hemodynamic response to nHBp. Individual dP/dt_{max} for a subset of 17 patients. CD: Conduction disturbance. EF: Ejection fraction. LVDD: left ventricle diastolic diameter. QRS_d: QRS duration. LVED: left ventricular electrical delay. LBBB: left bundle branch block. NICD: nonspecific intraventricular conduction disturbance.

Baseline						nHBp			
CD	LVDD [mm]	EF [%]	dP/dt _{max} [mm Hg/s]	QRS _d [ms]	LVED [ms]	dP/dt _{max} [mm Hg/s]	QRS _d [ms]	LVED [ms]	ΔdP/dt _{max} [mm Hg/s]
RBBB	73	23	703	119	81	698	109	66	-5
RBBB	55	35	1732	116	50	1744	92	72	12
LBBB	90	25	465	187	110	592	144	56	127
LBBB	57	25	960	144	94	1094	135	77	134
LBBB	83	20	326	193	135	481	151	69	155
LBBB	65	25	825	187	120	926	135	92	101
LBBB	81	22	801	115	112	817	125	76	16
LBBB	55	30	1241	147	89	1403	127	67	162
LBBB	58	25	936	137	82	991	125	43	55
LBBB	64	24	1106	145	132	1288	146	82	182
LBBB	60	38	1379	132	94	1610	77	37	231
LBBB	48	18	802	187	NA	991	135	NA	189
LBBB	72	35	1093	175	124	1190	129	74	97
LBBB	53	25	1175	142	105	1305	77	45	130
NICD	80	22	682	104	46	708	82	41	26
NICD	78	23	862	116	107	852	124	41	-10
NICD	62	27	745	101	86	694	114	54	-51

Table 4

ECG model. Estimated coefficients with standard error (SE), T-stats and p-values for the terms contributing to the LVED model. Cor_5 : Correlation shift (ms), A_{V_6} : area under lead V_6 , QRS_d : QRS duration (ms).

Fixed effects coefficients	Estimate	SE	t-Stat	p-Value
(Intercept)	17.19	14.44	1.19	0.239
QRS_d	0.47	0.08	5.63	8.9e-7
A_{V_6}	-0.06	0.01	-4.24	9.9e-5
Cor_5 :Gender	1.02	0.29	3.40	0.0013
Random effects coefficients	Type	Estimate	Lower	Upper
Intercept	Std	18.00	11.90	27.22

error dispersion defined as the 95% confidence intervals of the QRS_d model (98 ms) vs the ECG model (42 ms). Additionally, the error in the QRS model is biased, and not evenly distributed about zero, which in turn points at a handicap of the QRS model with respect to the ECG model.

Clinical application

In order to evidence the procedure for searching the optimal pacing site, Fig. 4 shows the crosscorrelation analysis for a LBBB case presenting two pacing sites (arrows vs asterisks). Baseline recording presented a LVED of 94 ms over a QRS 140 ms wide, while the nHB

Table 5

ECG vs QRS model. Likelihood ratio test comparing ECG model over QRS model. Note the significant improvement of the ECG model embodied in such a small p-value. DF: degrees of freedom, AIC: Akaike information criterion, BIC: Bayesian information criterion, LogLik: maximized log-likelihood, likelihood ratio test statistic for comparing ECG vs QRS models, LRStat: Likelihood ratio test statistic.

	DF	AIC	BIC	LogLik	LRStat	Δ DF	p-Value
QRS model	5	488.08	497.84	-239.04			
ECG model	6	471.59	483.29	-229.79	18.497	1	1.7e-05

paced at site 1 (arrows) presented a LVED of 79 ms and site 2 (asterisks) a LVED of 86 ms, both without appreciable change of the QRS duration (about 135 ms). Baseline R-peaks presented a time difference equal to 40 ms, in contrast to that of 16 ms for site 1 and 22 ms for site 2. This is a paradigmatic example where the aberrant QRS morphology and the misaligned R-peaks were corrected under nHB even though QRS duration did not substantially change. In addition, this example shows that even though QRS morphology varies very little from site 2 to site 1, differences in R peaks alignment can be finely tuned by crosscorrelation analysis. Since site 1 outperformed site 2 at R peak alignment, QRS segmentation and crosscorrelation analysis was displayed on those beats belonging to site 1 only.

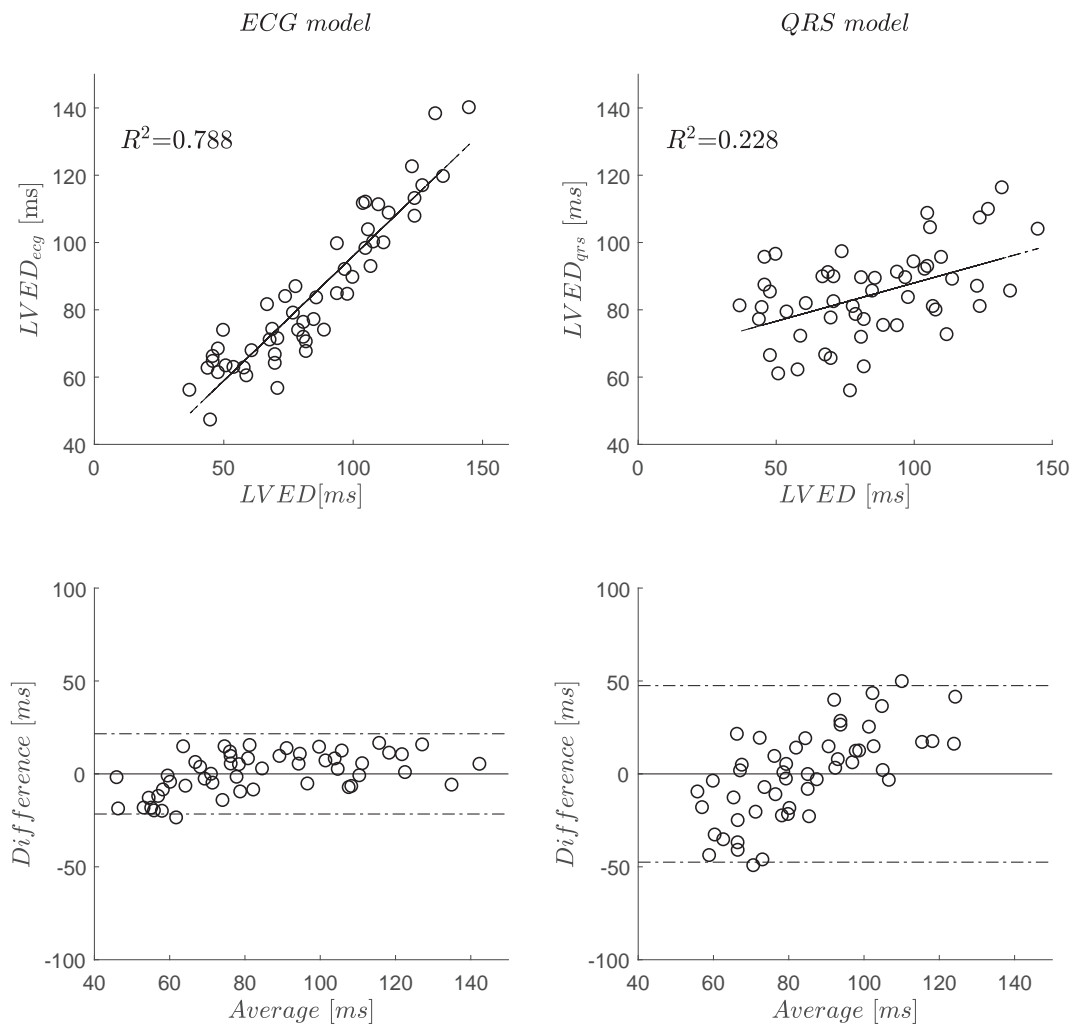


Fig. 3. QRS duration vs ECG model. Top: Model performance for $LVED_{QRS}$ (right panel) and $LVED_{ECG}$ (left panel) models for LVED estimation. Bottom: Bland-Altman plots for both models. Notice that the ECG model presents an unbiased estimation while the QRS_d model shows a bias not consistent throughout the average measures. It underestimates for short LVED values while it overestimates for long LVED values.

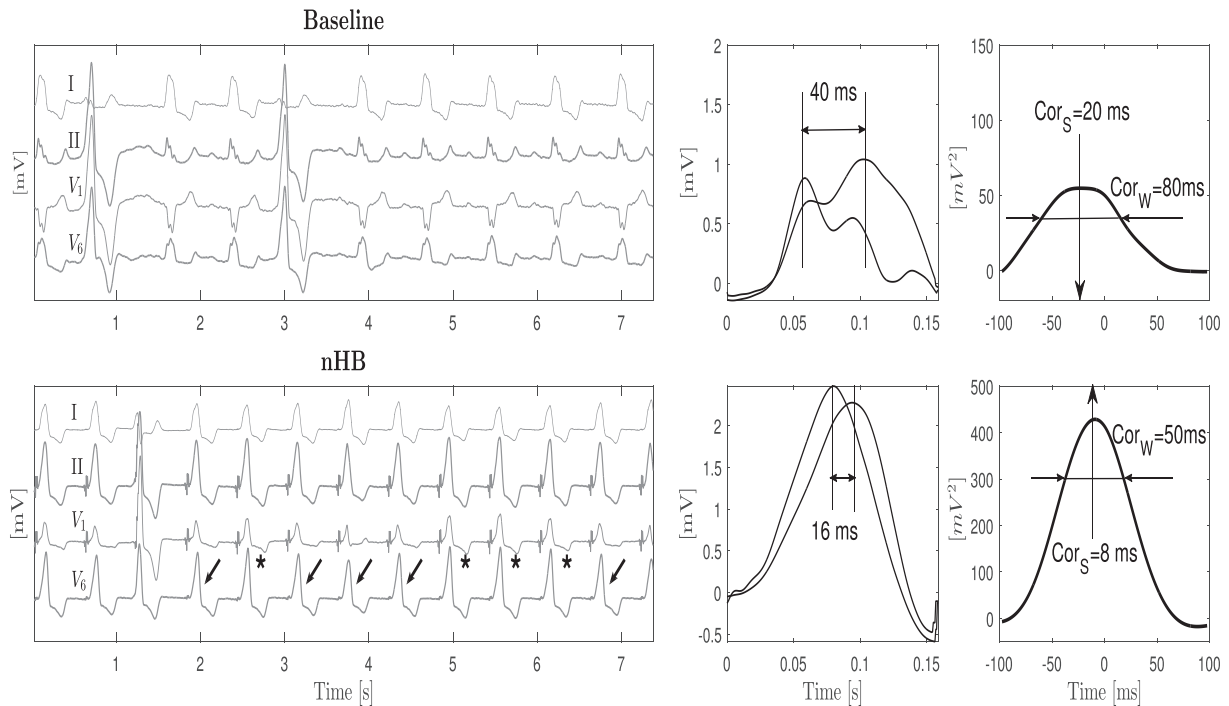


Fig. 4. Inpatient comparisons. Correlation analysis for paired baseline (top panel) and nHB stimulation (bottom panel) in a LBBB patient. Left) ECG traces recorded during EP. Middle) Superimposed QRS segments from leads II and V6 (II^{QRS} and V_6^{QRS}), respectively. Right) Correlation signal obtained from cross-correlating leads II and V_6 .

Discussion

We have presented a noninvasive model that predicts the left ventricular activation obtained through a catheter in the coronary venous system. With this ECG model, it is possible to optimize the site of pacing by searching for the area that minimizes the model's output, ensuring the earliest left ventricular activation.

Due to the acute nature of the experimental setup, our rationale relied on finding the electrocardiographic variables that best explained the late activation of the left ventricle measured invasively by coronary sinus mapping [12]. This late activation may be directly correlated to the conduction status within the left ventricle and therefore could serve as a marker of cardiac dyssynchrony. Since much evidence supports inter and intraventricular dyssynchrony as a predictor of CRT response better than QRS duration [17–19], the multivariable models proposed here would eventually help CRT indication as well. However, prospective long term follow up studies should be carried out in order to confirm this.

We pursued non-invasive LVED prediction based on the following experimental facts. Firstly, there exists evidence presenting LVED as a marker of intraventricular dyssynchrony [7] while a few studies have reported patients with non-LBBB ECG patterns and LVEDs exceeding 50% of their QRS durations [12,20]. In fact, NICD patients in this study applied to that case. Then, it could be speculated that those ECG features that best correlate to LVED would help unmask this concealed dyssynchrony. Finally, these patients would benefit from stimulation at these delayed areas by improving the hemodynamic response after CRT [7]. Secondly, by choosing an electrical outcome, a complete electrical model was determined. We believe that this coherence contributed to the obtained performance. Indeed, when we tried to explain a mechanical outcome with ECG parameters, the performance suffered dramatically ($R^2 = 27\%$, data not shown). This may be in line with findings from the PROSPECT study, such as the large variability in the analysis of mechanical dyssynchrony by echocardiography and the low area under the curve (AUC) in the prediction of the endpoints (<0.62 for all parameters) [21].

Also, the acute hemodynamic changes accompanied LVED improvements under nHBP, increasing dp/dt_{max} in 14 out of 17 patients (see Table 2). This is consistent with Catazariti et al., who compared acute hemodynamic data among selective and nonselective His bundle pacing and RVA pacing, showing improvement of LV function for the two former over RVA pacing, with no statistical difference when selective was compared to nonselective His bundle pacing [22]. Furthermore, Zanon et al. found that when pacing at the longest inpatient LVED, they obtained the best acute hemodynamic response in patients undergoing CRT [7].

However, a word of caution should be said regarding LVED in the particular cases of RBBBs and NICDs. By looking at Table 2, it is clear that advancing the left ventricle activation did not impact on a beneficial hemodynamic effect. On the contrary, it produced either no change or even decrements in dp/dt_{max} . Probably for these cases, the model should be used to keep LVED unchanged, in contrast to the remaining cases where LVED minimization is desirable.

Finally, leads II and V_6 produced the best LVED fits. We believe this fact shares anatomic foundations with Vereckei et al. [17]. In [17], time difference in intraseptal deflections of leads aV_F and V_5 were utilized as a marker of intraventricular dyssynchrony, based on their correlation with the anterior and posterior papillary muscles, which should contract simultaneously. We could think of leads II and V_6 as the same projection system, but slightly rotated to the left. Another remarkable coincidence is the ECG parameter that contributed to the model, Cor_S (see Table 3). As we explained above, Cor_S could be interpreted as a difference in intraseptal deflections when both lead morphologies show dominant R peaks.

Study limitations

Due to technical issues, only a reduced set of ECG leads were acquired, namely leads I and II in the frontal plane and leads V_1 and V_6 in the horizontal plane. It may seem quite a loss of information, but actually it is not. Remaining frontal leads (III, aV_R , aV_L and aV_F) are linearly dependent on the acquired leads, then they can easily be

computed from them. On the other hand, leads V_2 to V_5 represent intermediate projections between the two right and left extreme projections, V_1 and V_6 respectively, that account for the maximum variance of the electrical vector in the horizontal plane.

Conclusions

The inclusion of ECG interlead features obtained from cross-correlation of leads II and V_6 into models based only in QRS duration, substantially improved the prediction of LVED in patients with impaired intraventricular conduction. Thus, this ECG model served as a noninvasive, easy to implement tool for optimization of non-selective His bundle pacing site. Accordingly, it would also have potential for setting of AV delays or biventricular intervals in stimulation devices or even turn into a noninvasive dyssynchrony marker, although prospective long-term studies should confirm this.

References

- [1] Wilkoff B, Cook J, Epstein A, Greene H, Hallstrom A, Hsia H. et al. Dual chamber pacing or ventricular backup pacing in patients with an implantable defibrillator: the Dual Chamber and VVI Implantable Defibrillator (DAVID) trial. *JAMA* 2002;288:3115–23.
- [2] OKeefe JJ, Abuissa H, Jones P, Thompson R, Bateman T, McGhie A. Effect of chronic right ventricular apical pacing on left ventricular function. *Am J Cardiol* 2005;95:771–3.
- [3] Moss AJ, Hall WJ, Cannom DS, Klein H, Brown MW, Daubert JP. et al. Cardiac-resynchronization therapy for the prevention of heart-failure events. *N Engl J Med* 2009;361(14):1329–38.
- [4] Bristow MR, Saxon LA, Boehmer J, Krueger S, Kass DA, De Marco T. et al. Cardiac-resynchronization therapy with or without an implantable defibrillator in advanced chronic heart failure. *N Engl J Med* 2004;350(21):2140–50. PMID: 15152059. <https://doi.org/10.1056/NEJMoa032423>.
- [5] Singh J, Fan D, Heist E, Alabiad C, Taub C, Reddy V. et al. Left ventricular lead electrical delay predicts response to cardiac resynchronization therapy. *Heart Rhythm* 2006;3:1285–92.
- [6] Gold MR, Birgersdotter-Green U, Singh JP, Ellenbogen KA, Yu Y, Meyer TE. et al. The relationship between ventricular electrical delay and left ventricular remodeling with cardiac resynchronization therapy. *Eur Heart J* 2011;32(20):2516–24.
- [7] Zanon F, Baracca E, Pastore G, Fraccaro C, Roncon L, Aggjo S. et al. Determination of the longest inpatient left ventricular electrical delay may predict acute hemodynamic improvement in patients after cardiac resynchronization therapy: clinical perspective. *Circ Arrhythm Electrophysiol* 2014;7(3):377–83.
- [8] Barba-Pichardo R, Morriña-Vázquez P, Fernández-Gómez JM, Venegas-Gamero J, Herrera-Carranza M. Permanent His-bundle pacing: seeking physiological ventricular pacing. *Europace* 2010;12:527–33.
- [9] Lustgarten DL, Calame S, Crespo EM, Calame J, Robert Lobel, Spector PS. Electrical resynchronization induced by direct His-bundle pacing. *Heart Rhythm* 2010;7(1):15–21.
- [10] Occhetta E, Quirino G, Baduena L, Nappo R, Cavallino C, Facchini E. et al. Right ventricular septal pacing: safety and efficacy in a long term follow up. *JAMA* 2015;7:490–8.
- [11] Tung S, Lemaitre J. His bundle pacing: in pursuit of the “sweet spot”. *Pacing Clin Electrophysiol* 2015;38(5):537–9.
- [12] Bonomini MP, Ortega DF, Barja LD, Mangani NA, Paolucci A, Logarzo E. Electrical approach to improve left ventricular activation during right ventricle stimulation. *Med (B Aires)* 2017;77:7–12.
- [13] Ortega DF, Barja LD, Logarzo E, Mangani N, Paolucci A, Bonomini MP. Non-selective His bundle pacing with a biphasic waveform. enhancing septal resynchronization. *Europace* 2018;20(5):816–22.
- [14] Surawicz B, Childers R, Deal BJ, Gettes LS. AHA/ACCF/HRS recommendations for the standardization and interpretation of the electrocardiogram. *Circulation* 2009;119(10):e235–e240.
- [15] Martinez J, Almeida R, Olmos S, Rocha AP, Laguna P. A wavelet-based ECG delineator: evaluation on standard databases. *IEEE Trans Biomed Eng* 2004;51(4):570–81.
- [16] Sipahi I, Carrigan T, Rowland D, Stambler B, Fang J. Impact of QRS duration on clinical event reduction with cardiac resynchronization therapy: meta-analysis of randomized controlled trials. *Arch Intern Med* 2011;171(16):1454–62.
- [17] Vereckei A, Szelényi Z, Kutyaifa V, Gábor Szénási Z, Kiss M, Katona G. et al. Novel electrocardiographic dyssynchrony criteria improve patient selection for cardiac resynchronization therapy. *Europace* 2016; epub ahead of print.
- [18] Marek J, Saba S, Onishi T, Ryo K, Schwartzman D, Adelstein A. et al. Usefulness of echocardiographically guided left ventricular lead placement for cardiac resynchronization therapy in patients with intermediate QRS width and non-left bundle branch block morphology. *Am J Cardiol* 2014;113:107–16.
- [19] Hara H, Oyenuga O, Tanaka H, Adelstein E, Onishi T, McNamara D. et al. The relationship of QRS morphology and mechanical dyssynchrony to long-term outcome following cardiac resynchronization therapy. *Eur Heart J* 2012;33:2680–91.
- [20] Kandala J, Upadhyay G, Altman R, Parks K, Orencole M, Mela T. et al. QRS morphology, left ventricular lead location, and clinical outcome in patients receiving cardiac resynchronization therapy. *Eur Heart J* 2013;34(29):2252–62.
- [21] Chung ES, Leon AR, Tavazzi L, Sun JP, Nihoyannopoulos P, Merlino J. et al. Results of the Predictors of Response to CRT (PROSPECT) trial. *Circulation* 2008;117(20):2608–16.
- [22] Catanzariti D, Maines M, Manica A, Angheben C, Varbaro A, Vergara G. Permanent His-bundle pacing maintains long-term ventricular synchrony and left ventricular performance, unlike conventional right ventricular apical pacing. *Europace* 2013;15(4):546–53.